

Release Note – VBFNLO-2.6.0

K. Arnold¹, J. Bellm¹, G. Bozzi², F. Campanario¹, C. Englert³, B. Feigl¹, J. Frank¹,
T. Figy⁴, B. Jäger⁵, M. Kerner¹, M. Kubocz⁶, C. Oleari⁷, S. Palmer¹, M. Rauch¹,
H. Rzehak⁸, F. Schissler¹, O. Schlimpert¹, M. Spannowsky³, D. Zeppenfeld¹

¹ Institut für Theoretische Physik, Universität Karlsruhe, Karlsruhe Institute of
Technology, 76128 Karlsruhe, Germany

² Dipartimento di Fisica, Università di Milano and INFN, 20133 Milano, Italy

³ Institute for Particle Physics Phenomenology, University of Durham, Durham,
DH1 3LE, United Kingdom

⁴ School of Physics and Astronomy, The University of Manchester, Manchester,
M13 9PL, United Kingdom

⁵ Institut für Physik (THEP), Johannes-Gutenberg-Universität, 55099 Mainz, Germany

⁶ Institut für Theoretische Teilchenphysik und Kosmologie, RWTH Aachen University,
52056 Aachen, Germany

⁷ Dipartimento di Fisica, Università di Milano-Bicocca and INFN, Sezione di
Milano-Bicocca, 20126 Milano, Italy

⁸ CERN, CH-1211 Geneva 23, Switzerland (on leave from: Physikalisches Institut
Albert-Ludwigs-Universität Freiburg, Hermann-Herder-Str. 3, 79104 Freiburg im
Breisgau, Germany)

Abstract

VBFNLO is a flexible parton level Monte Carlo program for the simulation of vector boson fusion (VBF), double and triple vector boson (plus jet) production in hadronic collisions at next-to-leading order (NLO) in the strong coupling constant, as well as Higgs boson plus two jet production via gluon fusion at the one-loop level. This note briefly describes the main additional features and processes that have been added in the new release – VBFNLO VERSION 2.6.0. At NLO QCD diboson production ($W\gamma$, WZ , ZZ , $Z\gamma$ and $\gamma\gamma$), same-sign W pair production via vector boson fusion and the process $W\gamma\gamma j$ have been implemented (for which one-loop tensor integrals up to six-point functions are included). In addition, gluon induced diboson production can be studied separately at the leading order (one-loop) level. The diboson processes WW , WZ and $W\gamma$ can be run with anomalous gauge boson couplings, and anomalous couplings between a Higgs and a pair of gauge bosons is included in WW , ZZ , $Z\gamma$ and $\gamma\gamma$ diboson production. The code has also been extended to include anomalous gauge boson couplings for single vector boson production via VBF, and a spin-2 model has been implemented for diboson pair production via vector boson fusion.

1 INTRODUCTION

VBFNLO [1, 2] is a flexible Monte Carlo (MC) program for vector boson fusion (VBF), double and triple vector boson (plus jet) production processes at NLO QCD accuracy. The electroweak corrections to Higgs boson production via VBF have been included. In addition, the simulation of \mathcal{CP} -even and \mathcal{CP} -odd Higgs boson production in gluon fusion, associated with two additional jets, is implemented at the (one-loop) LO QCD level. VBFNLO can be run in the MSSM, and anomalous couplings of the Higgs boson and gauge bosons have been implemented for certain processes. Additionally, two Higgsless extra dimension models are included – the Warped Higgsless scenario and a Three-Site Higgsless Model – for selected processes.

Further information, and the latest version of the code, can be found on the VBFNLO webpage

<http://www-itp.particle.uni-karlsruhe.de/vbfnlo/>

A complete process list is given in Appendix A.

2 New processes

The latest version of VBFNLO has several new processes implemented at NLO QCD.

2.1 Same sign W pair production via VBF

Same sign W pair production with two jets via vector boson fusion [3] has been included in VBFNLO 2.6.0. This process is potentially sensitive to new physics signals and, as it gives rise to same sign dilepton final states, it is also a background to new physics scenarios. To distinguish potential signatures of physics beyond the Standard Model from the effect of higher order corrections, precise theoretical predictions are essential. Although the QCD corrections to the integrated cross sections were found to be relatively small, their effect on several distributions is appreciable. When NLO QCD corrections are taken into account, the residual scale uncertainties are at the 2.5% level. The new process IDs are given in Table 1.

PROCID	PROCESS
250	$p\bar{p}^{(-)} \rightarrow W^+W^+ jj \rightarrow \ell_1^+ \nu_{\ell_1} \ell_2^+ \nu_{\ell_2} jj$
260	$p\bar{p}^{(-)} \rightarrow W^-W^- jj \rightarrow \ell_1^- \bar{\nu}_{\ell_1} \ell_2^- \bar{\nu}_{\ell_2} jj$

Table 1: *New process IDs for diboson + 2 jet production via vector boson fusion at NLO QCD accuracy.*

2.2 Diboson production and gluon-induced contributions

A good understanding of diboson processes at the LHC is essential, as not only do they allow the study of the Standard Model’s gauge structure, but they also provide a background to Higgs boson and new physics searches. Anomalous triple gauge boson couplings are included in the WZ and $W\gamma$ processes¹. (For contributions from anomalous HVV couplings in gluon induced processes – Fig. 1 – see below.) The new processes are included at NLO QCD accuracy under the process IDs shown in Table 2.

PROCID	PROCESS	BSM
310	$p\bar{p} \xrightarrow{(-)} W^+Z \rightarrow \ell_1^+ \nu_{\ell_1} \ell_2^+ \ell_2^-$	} anomalous VVV couplings
320	$p\bar{p} \xrightarrow{(-)} W^-Z \rightarrow \ell_1^- \bar{\nu}_{\ell_1} \ell_2^+ \ell_2^-$	
330	$p\bar{p} \xrightarrow{(-)} ZZ \rightarrow \ell_1^- \ell_1^+ \ell_2^- \ell_2^+$	anomalous HVV couplings
340	$p\bar{p} \xrightarrow{(-)} W^+\gamma \rightarrow \ell_1^+ \nu_{\ell_1} \gamma$	} anomalous VVV couplings
350	$p\bar{p} \xrightarrow{(-)} W^-\gamma \rightarrow \ell_1^- \bar{\nu}_{\ell_1} \gamma$	
360	$p\bar{p} \xrightarrow{(-)} Z\gamma \rightarrow \ell_1^- \ell_1^+ \gamma$	} anomalous HVV couplings
370	$p\bar{p} \xrightarrow{(-)} \gamma\gamma$	

Table 2: *Process IDs for the new diboson production processes at NLO QCD accuracy.*

In addition to the NLO QCD corrections, the gluon-induced fermionic loop processes can be included in those processes with neutral final states (including WW production, which was already implemented in VBFNLO, with process ID 300). Both continuum production via box diagrams as well as production via an s-channel Higgs boson resonance (shown in Fig. 1) are available, with full interference effects.

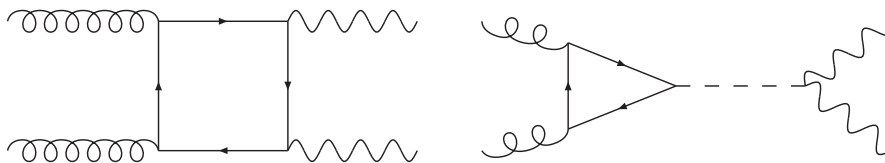


Figure 1: Gluon-induced contributions to diboson production.

The `vbfno.dat` flag `FERMIONLOOP` controls these contributions:

- 0 switches off these processes
- 1 includes only the box contribution
- 2 includes only diagrams via an s-channel Higgs resonance
- 3 includes both contributions including interference effects.

¹As in the rest of VBFNLO, no neutral triple gauge couplings are included.

Although these contributions are formally of higher order, their effect can still be significant. Anomalous couplings between a Higgs boson and a pair of gauge bosons can be included in those processes with neutral final states. The gluon-induced loop diagrams can be studied separately in the new release of VBFNLO using the process IDs of Table 3 and the executable `ggflo`.

PROCID	PROCESS	BSM
4300	$gg \rightarrow W^+W^- \rightarrow \ell_1^+ \nu_{\ell_1} \ell_2^- \bar{\nu}_{\ell_2}$	} anomalous HVV couplings
4330	$gg \rightarrow ZZ \rightarrow \ell_1^- \ell_1^+ \ell_2^- \ell_2^+$	
4360	$gg \rightarrow Z\gamma \rightarrow \ell_1^- \ell_1^+ \gamma$	
4370	$gg \rightarrow \gamma\gamma$	

Table 3: *Process IDs for gluon induced diboson production at LO (one-loop) QCD.*

2.3 Triple vector boson production in association with a hadronic jet

Finally, the triboson plus jet processes given in Table 4 have also been included at NLO QCD level² [4]. As a process involving multiple electroweak bosons and jets, this is an important channel in which to compare experimental data with the predictions of the Standard Model. The NLO QCD corrections to the total cross section are sizeable, and have a non-trivial phasespace dependence.

PROCID	PROCESS
800	$p\bar{p}^{(-)} \rightarrow W^+ \gamma\gamma j \rightarrow \ell^+ \nu_{\ell} \gamma\gamma j$
810	$p\bar{p}^{(-)} \rightarrow W^- \gamma\gamma j \rightarrow \ell^- \bar{\nu}_{\ell} \gamma\gamma j$

Table 4: *Process IDs for triboson production in association with a hadronic jet at NLO QCD.*

3 New features

In addition to the new processes described above, several existing procedures have been extended and new features added.

²These processes are disabled by default and must be enabled at compilation using the `configure` option `--enable-processes=all` or `--enable-processes=tribosonjet`.

3.1 Tensor reduction routines

The tensor reduction routines for up to 4 external legs have been extended for general kinematics. Three and four point tensor integrals are extended to deal with Rank 3 and Rank 4 integrals, respectively. Furthermore, one-loop tensor reduction routines for up to 6 external legs have been included for the massless case. The tensor integrals are implemented following Ref. [5] and can be found in the directory `loops/TenRed`.

3.2 Anomalous couplings

Anomalous gauge boson couplings have been implemented for single vector boson production via VBF, which have been seen to have an effect on some distributions [6], such as the azimuthal angle separation of the tagging jets. The existing diboson process $pp \rightarrow WW$ has been modified to include anomalous VVV couplings, as well as anomalous HVV couplings in the gluon-induced contributions. The relevant process IDs are given in Table 5. To run VBFNLO with anomalous couplings, the switch `ANOM_CPL` in the input file `vbfnlo.dat` must be switched to `true`. The anomalous coupling parameters are then input via `anomV.dat` or (for HVV couplings) `anom_HVV.dat`.

PROCID	PROCESS	BSM
120	$pp^{(-)} \rightarrow Z jj \rightarrow \ell^+ \ell^- jj$	} anomalous couplings
121	$pp^{(-)} \rightarrow Z jj \rightarrow \nu_\ell \bar{\nu}_\ell jj$	
130	$pp^{(-)} \rightarrow W^+ jj \rightarrow \ell^+ \nu_\ell jj$	
140	$pp^{(-)} \rightarrow W^- jj \rightarrow \ell^- \bar{\nu}_\ell jj$	
150	$pp^{(-)} \rightarrow \gamma jj$	
300	$pp^{(-)} \rightarrow W^+ W^- \rightarrow \ell_1^+ \nu_{\ell_1} \ell_2^- \bar{\nu}_{\ell_2}$	anomalous VVV and HVV couplings

Table 5: *Process IDs for existing processes which have been extended to include anomalous couplings.*

3.3 Spin-2 model

A spin-2 model has been implemented, using an effective Lagrangian to describe the interactions of spin-2 particles with electroweak gauge bosons for two cases: an isospin singlet spin-2 state and a spin-2 triplet, as described in Ref. [7]. This spin-2 model is implemented for diboson plus two jets production via vector boson fusion ($pp \rightarrow W^+ W^- jj$, $pp \rightarrow ZZjj$ and $pp \rightarrow WZjj$, process IDs 200 - 230). For these processes a spin-2 resonance is included in addition to the Standard Model diagrams (i.e. both Higgs boson and spin-2 diagrams are calculated).

The file `spin2coupl.dat` is used to set the parameters for the spin-2 models. It is read if the switch `SPIN2` in `vbfnlo.dat` is set to `true`, and will only run if the spin-2 models were enabled at compilation using the `configure` option `--enable-spin2`.

For the singlet spin-2 field, $T^{\mu\nu}$, the effective Lagrangian is

$$\mathcal{L}_{\text{singlet}} = \frac{1}{\Lambda} T_{\mu\nu} \left(f_1 B^{\alpha\nu} B_\alpha^\mu + f_2 W_i^{\alpha\nu} W_\alpha^{i,\mu} + f_3 \widetilde{B}^{\alpha\nu} B_\alpha^\mu + f_4 \widetilde{W}_i^{\alpha\nu} W_\alpha^{i,\mu} + 2f_5 (D^\mu \Phi)^\dagger (D^\nu \Phi) \right), \quad (1)$$

and for the spin-2 triplet field, $T_j^{\mu\nu}$, the effective Lagrangian is given by

$$\mathcal{L}_{\text{triplet}} = \frac{1}{\Lambda} T_{\mu\nu j} \left(f_6 (D^\mu \Phi)^\dagger \sigma^j (D^\nu \Phi) + f_7 W_\alpha^{j,\mu} B^{\alpha\nu} \right), \quad (2)$$

where W and B are the usual electroweak field strength tensors, \widetilde{W} and \widetilde{B} the dual field strength tensors, Φ is the Higgs field and D^μ is the covariant derivative. f_i are variable coupling parameters and Λ is the characteristic energy scale of the new physics.

In order to preserve unitarity, a formfactor is introduced to multiply the amplitudes. The formfactor has the form:

$$f(q_1^2, q_2^2, p_{\text{sp}2}^2) = \left(\frac{\Lambda_{ff}^2}{|q_1^2| + \Lambda_{ff}^2} \cdot \frac{\Lambda_{ff}^2}{|q_2^2| + \Lambda_{ff}^2} \cdot \frac{\Lambda_{ff}^2}{|p_{\text{sp}2}^2| + \Lambda_{ff}^2} \right)^{n_{ff}}. \quad (3)$$

Here $p_{\text{sp}2}^2$ is the invariant mass of a virtual s-channel spin-2 particle and $q_{1,2}^2$ are the invariant masses of the electroweak bosons. The energy scale Λ_{ff} and the exponent n_{ff} describe the scale of the cutoff and the suppression power.

The input parameters used by VBFNLO are

- **F1, F2, F3, F4, F5**: Coupling parameters for the spin-2 singlet field. Default values are F1=F2=F5=1, F3=F4=0.
- **F6, F7**: Coupling parameters for the spin-2 triplet field. Default values are set to 1.
- **LAMBDA**: Energy scale of the couplings in GeV. Default value is 1500 GeV.
- **LAMBDAFF**: Energy scale of the formfactor in GeV. Default value is 3000 GeV.
- **NFF**: Exponent of the formfactor. Default value is 4.

Note that a graviton corresponds to F1=F2=F5=1 and F3=F4=F6=F7=0.

VBFNLO also needs the masses and branching ratios (into SM gauge bosons) of the spin-2 particles.

- **SP2MASS**: Mass of the spin-2 singlet particle in GeV. Default value is 1000 GeV.
- **MSP2TRIPPM**: Mass of charged spin-2 triplet particles in GeV. Default value is 1000 GeV.
- **MSP2TRIPN**: Mass of neutral spin-2 triplet particle in GeV. Default value is 1000 GeV.
- **BRRAT**: Branching ratio into SM gauge bosons for spin-2 singlet particle. Default value is 1.
- **BRRATTRIPPM**: Branching ratio into SM gauge bosons for charged spin-2 triplet particles. Default value is 1.
- **BRRATTRIPN**: Branching ratio into SM gauge bosons for neutral spin-2 triplet particle. Default value is 1.

A new process $pp \rightarrow \gamma\gamma jj$ (Table 6) has been added which includes only the resonant spin-2 diagrams – this can be compared to the existing process of Higgs boson production via VBF, where the Higgs decays into photons (process ID 101). The default values given above are intended for processes 200-230. Corresponding values for light spin-2 resonances in process 191 can be found in Ref. [7]³.

PROCID	PROCESS	BSM
191	$p\bar{p}^{(-)} \rightarrow S_2 jj \rightarrow \gamma\gamma jj$	spin-2 resonant production only

Table 6: *Process ID for production of a spin-2 particle S_2 with 2 jets via vector boson fusion at NLO QCD accuracy.*

3.4 Histograms

The error calculation for the real emission output can now be controlled via the input file `histograms.dat`. VBFNLO can calculate the Monte Carlo error for each bin and output this to the raw histogram data output for 1D and 2D histograms. For the gnuplot histogram output only the 1D histograms can display the error bars⁴.

- `CALC_ERROR_GNUPLOT`: Enable or disable y-error bars in 1D gnuplot histograms. Default is `false`.
- `CALC_ERROR_1D`: Enable or disable y-error bars in raw 1D histogram output. Default is `true`.
- `CALC_ERROR_2D`: Enable or disable z-error bars in raw 2D histogram output. Default is `false`.

Furthermore, VBFNLO uses a smearing between adjacent bins to avoid artefacts at NLO when the real emission kinematics and the corresponding subtraction term fall into different bins. As this can lead to remnants at the sharp edges caused by cuts, the smearing can be switched off.

- `SMEARING`: Enable or disable smearing. Default is `true`.
- `SMEAR_VALUE`: Set the bin fraction where the bin smearing is active. The part that is put to the next bin becomes larger when the x-value is closer to a bin border. Default is `0.2`.

³Note that in Ref. [7] this process is referred to as process 240.

⁴Error calculation is not implemented for the other (ROOT or TOPDRAWER) histogram formats.

3.5 SUSY options for electroweak corrections

When running VBFNLO in the MSSM, it is now possible to set the mass of the Higgs bosons in the electroweak loops to either their tree-level value or their corrected value, using the flag `MH_LOOPS` in `susy.dat`.

In some areas of the MSSM parameter space, the electroweak loop corrections can be the dominant contribution to the cross section. In this case, the squared electroweak corrections from the (s)fermion corrections are important and can be included in VBFNLO using the `susy.dat` flag `LOOPSQR_SWITCH`. If set to `true` the amplitude is given by

$$|\mathcal{M}_{\text{Born}}|^2 + 2\Re[\mathcal{M}_{\text{Born}}^* \mathcal{M}_{\text{loop}}] + |\mathcal{M}_{(\text{s})\text{fermion loop}}|^2. \quad (4)$$

Note that the loop squared component is only added if $|\mathcal{M}_{(\text{s})\text{fermion loop}}|$ is greater than 10% of $|\mathcal{M}_{\text{Born}}|$.

4 Other changes

Since the previous release, VERSION 2.5.0, some changes have been made that alter previous results (events, cross sections and distributions).

4.1 Allowed virtuality of resonance

In the phasespace generators, the allowed range of the virtuality of a resonance of intermediate vector bosons has been increased. This mainly affects processes where an intermediate Z boson decays into a pair of neutrinos – i.e.

- $pp \rightarrow Hjj \rightarrow ZZjj \rightarrow \ell^+ \ell^- \nu \bar{\nu} jj$ via vector boson fusion (process ID 107) and gluon fusion (process ID 4107)
- $pp \rightarrow Hjjj \rightarrow ZZjjj \rightarrow \ell^+ \ell^- \nu \bar{\nu} jjj$ (process ID 117)
- $pp \rightarrow H\gamma jj \rightarrow ZZ\gamma jj \rightarrow \ell^+ \ell^- \nu \bar{\nu} \gamma jj$ (process ID 2107)
- $pp \rightarrow ZZjj \rightarrow \ell^+ \ell^- \nu \bar{\nu} jj$ (process ID 211)

This not only affects the cross sections for these processes, but also means that the events produced by VBFNLO-2.6.0 will differ from those produced by VBFNLO-2.5, even if the same random numbers are used.

4.2 Matrix element $H \rightarrow ZZ \rightarrow 4\ell$

A bug was found and fixed in the implementation of the matrix element calculating the decay $H \rightarrow ZZ \rightarrow 4\ell$.

4.3 Anomalous couplings

Several changes have been made to the implementation of the anomalous couplings. For Higgs production via vector boson fusion (process IDs 100-107) the variable `TREEFAC`, which multiplies the Standard Model contribution to the tree-level HVV couplings, has been corrected and altered – now, separate factors for HZZ and HWW are input (`TREEFACZ` and `TREEFACW` respectively).

When working with anomalous HVV couplings two types of formfactors can be applied which model effective, momentum dependent HVV vertices, motivated by new physics entering with a large scale Λ at loop level. Corrections to the HVV formfactor F_2 , where

$$F_2 = -2\Lambda^2 C_0(q_1^2, q_2^2, (q_1 + q_2)^2, \Lambda^2). \quad (5)$$

(where the q_i are the momenta of the vector bosons and C_0 is the scalar one-loop three point function in the notation of Ref. [8]) have been made. The implementation of the parametrization described by `PARAMETR3` – where the input determining the anomalous couplings is in terms of the dimension-6 operators (\mathcal{O}_W , \mathcal{O}_B , \mathcal{O}_{WW} and \mathcal{O}_{BB} , see [9, 10]) – has also been corrected.

If anomalous triple (and quartic) gauge boson couplings are being studied, a formfactor, given by

$$F = \left(1 + \frac{s}{\Lambda^2}\right)^{-p}, \quad (6)$$

can be applied in order to preserve unitarity, where Λ is again the scale of new physics. The momentum dependence of an applied formfactor (i.e. s) is now universal for each phase space point, with the invariant mass of the bosons as the scale. This ensures the proper cancellations for anomalous contributions and affects both the cross sections and the distributions significantly.

The values of the formfactor scale Λ and suppression p can be set to different values for each input describing the triboson couplings. In the parameterization `TRIANOM = 2` of the L3 Collaboration [11], the formfactor scales for $\Delta\kappa_\gamma$ and $\Delta\kappa_Z$ are now separately set, and the consistency of related parameters (i.e. Δg_1^Z , $\Delta\kappa_\gamma$ and $\Delta\kappa_Z$) is enforced when formfactors are applied.

When processes involving resonant Higgs diagrams (e.g. WWW production) are studied with anomalous couplings, the Higgs width is now calculated with the appropriate anomalous HVV couplings (the anomalous HVV couplings in the production amplitudes were taken into account in previous versions of `VBFNLO`). Various corrections have also been made to the anomalous triboson couplings in diboson plus jet processes (these were incorporated into the intermediate release `VBFNLO 2.5.3`).

4.4 VBF Higgs boson production in association with three jets

A small bug was found and fixed in the calculation of the processes $pp \rightarrow Hjjj$, with process IDs 110-117.

Acknowledgments

We are grateful to Simon Plätzer, Manuel Bähr, Martin Brieg, Florian Geyer, Nicolas Greiner, Christoph Hackstein, Vera Hankele, Gunnar Klämke, Stefan Prestel and Malgorzata Worek for their past contributions to the `VBFNLO` code. We would also like to thank Julien Baglio for help in testing the code. TF would like to thank the North American Foundation for The University of Manchester and George Rigg for their financial support.

References

- [1] K. Arnold, M. Bahr, G. Bozzi *et al.*, “VBFNLO: A parton level Monte Carlo for processes with electroweak bosons”, *Comput. Phys. Commun.* **180** (2009) 1661-1670, [arXiv:0811.4559](#).
- [2] K. Arnold, J. Bellm, G. Bozzi *et al.*, “VBFNLO: A parton level Monte Carlo for processes with electroweak bosons – Manual for Version 2.5.0,” [arXiv:1107.4038](#).
- [3] B. Jager, C. Oleari and D. Zeppenfeld, “Next-to-leading order QCD corrections to W^+W^+jj and W^-W^-jj production via weak-boson fusion,” *Phys. Rev.* **D80** (2009) 034022, [arXiv:0907.0580](#).
- [4] F. Campanario, C. Englert, M. Rauch and D. Zeppenfeld, “Precise predictions for $W\gamma\gamma$ +jet production at hadron colliders,” *Phys. Lett. B* **704** (2011) 515, [arXiv:1106.4009](#).
- [5] F. Campanario, “Towards $pp \rightarrow VVjj$ at NLO QCD: Bosonic contributions to triple vector boson production plus jet,” *JHEP* **1110** (2011) 070, [arXiv:1105.0920](#).
- [6] B. Jager, “Next-to-leading order QCD corrections to photon production via weak-boson fusion”, *Phys. Rev.* **D81** (2010) 114016, [arXiv:1004.0825](#).
- [7] J. Frank, “Spin-2 Resonances in Vector Boson Fusion Processes at the LHC”, Diploma Thesis, ITP Karlsruhe 2011, <http://www-itp.particle.uni-karlsruhe.de/diplomatheses.en.shtml>.
- [8] G. Passarino and M. J. G. Veltman, “One Loop Corrections for e^+e^- Annihilation into $\mu^+\mu^-$ in the Weinberg Model”, *Nucl. Phys.* **B160** (1979) 151.
- [9] K. Hagiwara, R. Szalapski and D. Zeppenfeld, “Anomalous Higgs boson production and decay”, *Phys. Lett.* **B318** (1993) 155, [hep-ph/9308347](#).
- [10] K. Hagiwara, S. Ishihara, R. Szalapski and D. Zeppenfeld, “Low-energy effects of new interactions in the electroweak boson sector”, *Phys. Rev.* **D48** (1993) 2182.
- [11] L3 Collaboration, “Search for anomalous couplings in the Higgs sector at LEP”, *Phys. Lett.* **B589** (2004) 89, [hep-ex/0403037](#).

Appendix A: Process List

The following is a complete list of all processes available in VBFNLO, including any Beyond the Standard Model (BSM) effects that are implemented. Firstly, the processes that are accessed via the `vbfno` executable are given.

PROCID	PROCESS	BSM
100	$p\bar{p} \rightarrow H jj$	} anomalous HVV couplings, MSSM
101	$p\bar{p} \rightarrow H jj \rightarrow \gamma\gamma jj$	
102	$p\bar{p} \rightarrow H jj \rightarrow \mu^+\mu^- jj$	
103	$p\bar{p} \rightarrow H jj \rightarrow \tau^+\tau^- jj$	
104	$p\bar{p} \rightarrow H jj \rightarrow b\bar{b} jj$	
105	$p\bar{p} \rightarrow H jj \rightarrow W^+W^- jj \rightarrow \ell_1^+ \nu_{\ell_1} \ell_2^- \bar{\nu}_{\ell_2} jj$	
106	$p\bar{p} \rightarrow H jj \rightarrow ZZ jj \rightarrow \ell_1^+ \ell_1^- \ell_2^+ \ell_2^- jj$	
107	$p\bar{p} \rightarrow H jj \rightarrow ZZ jj \rightarrow \ell_1^+ \ell_1^- \nu_{\ell_2} \bar{\nu}_{\ell_2} jj$	
110	$p\bar{p} \rightarrow H jjj$	
111	$p\bar{p} \rightarrow H jjj \rightarrow \gamma\gamma jjj$	
112	$p\bar{p} \rightarrow H jjj \rightarrow \mu^+\mu^- jjj$	
113	$p\bar{p} \rightarrow H jjj \rightarrow \tau^+\tau^- jjj$	
114	$p\bar{p} \rightarrow H jjj \rightarrow b\bar{b} jjj$	
115	$p\bar{p} \rightarrow H jjj \rightarrow W^+W^- jjj \rightarrow \ell_1^+ \nu_{\ell_1} \ell_2^- \bar{\nu}_{\ell_2} jjj$	
116	$p\bar{p} \rightarrow H jjj \rightarrow ZZ jjj \rightarrow \ell_1^+ \ell_1^- \ell_2^+ \ell_2^- jjj$	
117	$p\bar{p} \rightarrow H jjj \rightarrow ZZ jjj \rightarrow \ell_1^+ \ell_1^- \nu_{\ell_2} \bar{\nu}_{\ell_2} jjj$	
2100	$p\bar{p} \rightarrow H\gamma jj$	
2101	$p\bar{p} \rightarrow H\gamma jj \rightarrow \gamma\gamma\gamma jj$	
2102	$p\bar{p} \rightarrow H\gamma jj \rightarrow \mu^+\mu^-\gamma jj$	
2103	$p\bar{p} \rightarrow H\gamma jj \rightarrow \tau^+\tau^-\gamma jj$	
2104	$p\bar{p} \rightarrow H\gamma jj \rightarrow b\bar{b}\gamma jj$	
2105	$p\bar{p} \rightarrow H\gamma jj \rightarrow W^+W^-\gamma jj \rightarrow \ell_1^+ \nu_{\ell_1} \ell_2^- \bar{\nu}_{\ell_2} \gamma jj$	
2106	$p\bar{p} \rightarrow H\gamma jj \rightarrow ZZ\gamma jj \rightarrow \ell_1^+ \ell_1^- \ell_2^+ \ell_2^- \gamma jj$	
2107	$p\bar{p} \rightarrow H\gamma jj \rightarrow ZZ\gamma jj \rightarrow \ell_1^+ \ell_1^- \nu_{\ell_2} \bar{\nu}_{\ell_2} \gamma jj$	

PROCID	PROCESS	BSM
120	$p\bar{p}^{(-)} \rightarrow Z jj \rightarrow \ell^+ \ell^- jj$	} anomalous couplings
121	$p\bar{p}^{(-)} \rightarrow Z jj \rightarrow \nu_\ell \bar{\nu}_\ell jj$	
130	$p\bar{p}^{(-)} \rightarrow W^+ jj \rightarrow \ell^+ \nu_\ell jj$	
140	$p\bar{p}^{(-)} \rightarrow W^- jj \rightarrow \ell^- \bar{\nu}_\ell jj$	
150	$p\bar{p}^{(-)} \rightarrow \gamma jj$	
191	$p\bar{p}^{(-)} \rightarrow S_2 jj \rightarrow \gamma\gamma jj$	only spin-2 resonant production
200	$p\bar{p}^{(-)} \rightarrow W^+ W^- jj \rightarrow \ell_1^+ \nu_{\ell_1} \ell_2^- \bar{\nu}_{\ell_2} jj$	} anomalous couplings, Kaluza-Klein & spin-2 models } Kaluza-Klein models, spin-2 models
210	$p\bar{p}^{(-)} \rightarrow ZZ jj \rightarrow \ell_1^+ \ell_1^- \ell_2^+ \ell_2^- jj$	
211	$p\bar{p}^{(-)} \rightarrow ZZ jj \rightarrow \ell_1^+ \ell_1^- \nu_{\ell_2} \bar{\nu}_{\ell_2} jj$	
220	$p\bar{p}^{(-)} \rightarrow W^+ Z jj \rightarrow \ell_1^+ \nu_{\ell_1} \ell_2^+ \ell_2^- jj$	
230	$p\bar{p}^{(-)} \rightarrow W^- Z jj \rightarrow \ell_1^- \bar{\nu}_{\ell_1} \ell_2^+ \ell_2^- jj$	
250	$p\bar{p}^{(-)} \rightarrow W^+ W^+ jj \rightarrow \ell_1^+ \nu_{\ell_1} \ell_2^+ \nu_{\ell_2} jj$	
260	$p\bar{p}^{(-)} \rightarrow W^- W^- jj \rightarrow \ell_1^- \bar{\nu}_{\ell_1} \ell_2^- \bar{\nu}_{\ell_2} jj$	
300	$p\bar{p}^{(-)} \rightarrow W^+ W^- \rightarrow \ell_1^+ \nu_{\ell_1} \ell_2^- \bar{\nu}_{\ell_2}$	anomalous VVV and HVV couplings
310	$p\bar{p}^{(-)} \rightarrow W^+ Z \rightarrow \ell_1^+ \nu_{\ell_1} \ell_2^+ \ell_2^-$	} anomalous VVV couplings
320	$p\bar{p}^{(-)} \rightarrow W^- Z \rightarrow \ell_1^- \bar{\nu}_{\ell_1} \ell_2^+ \ell_2^-$	
330	$p\bar{p}^{(-)} \rightarrow ZZ \rightarrow \ell_1^- \ell_1^+ \ell_2^- \ell_2^+$	anomalous HVV couplings
340	$p\bar{p}^{(-)} \rightarrow W^+ \gamma \rightarrow \ell_1^+ \nu_{\ell_1} \gamma$	} anomalous VVV couplings
350	$p\bar{p}^{(-)} \rightarrow W^- \gamma \rightarrow \ell_1^- \bar{\nu}_{\ell_1} \gamma$	
360	$p\bar{p}^{(-)} \rightarrow Z \gamma \rightarrow \ell_1^- \ell_1^+ \gamma$	} anomalous HVV couplings
370	$p\bar{p}^{(-)} \rightarrow \gamma\gamma$	

PROCID	PROCESS	BSM
400	$p\bar{p} \rightarrow W^+W^-Z \rightarrow \ell_1^+\nu_{\ell_1}\ell_2^-\bar{\nu}_{\ell_2}\ell_3^+\ell_3^-$	} anomalous couplings, Kaluza-Klein models
410	$p\bar{p} \rightarrow ZZW^+ \rightarrow \ell_1^+\ell_1^-\ell_2^+\ell_2^-\ell_3^+\nu_{\ell_3}$	
420	$p\bar{p} \rightarrow ZZW^- \rightarrow \ell_1^+\ell_1^-\ell_2^+\ell_2^-\ell_3^-\bar{\nu}_{\ell_3}$	
430	$p\bar{p} \rightarrow W^+W^-W^+ \rightarrow \ell_1^+\nu_{\ell_1}\ell_2^-\bar{\nu}_{\ell_2}\ell_3^+\nu_{\ell_3}$	
440	$p\bar{p} \rightarrow W^-W^+W^- \rightarrow \ell_1^-\bar{\nu}_{\ell_1}\ell_2^+\nu_{\ell_2}\ell_3^-\bar{\nu}_{\ell_3}$	
450	$p\bar{p} \rightarrow ZZZ \rightarrow \ell_1^-\ell_1^+\ell_2^-\ell_2^+\ell_3^-\ell_3^+$	
460	$p\bar{p} \rightarrow W^-W^+\gamma \rightarrow \ell_1^-\bar{\nu}_{\ell_1}\ell_2^+\nu_{\ell_2}\gamma$	
470	$p\bar{p} \rightarrow ZZ\gamma \rightarrow \ell_1^-\ell_1^+\ell_2^-\ell_2^+\gamma$	
480	$p\bar{p} \rightarrow W^+Z\gamma \rightarrow \ell_1^+\nu_{\ell_1}\ell_2^-\ell_2^+\gamma$	
490	$p\bar{p} \rightarrow W^-Z\gamma \rightarrow \ell_1^-\bar{\nu}_{\ell_1}\ell_2^-\ell_2^+\gamma$	
500	$p\bar{p} \rightarrow W^+\gamma\gamma \rightarrow \ell^+\nu_{\ell}\gamma\gamma$	
510	$p\bar{p} \rightarrow W^-\gamma\gamma \rightarrow \ell^-\bar{\nu}_{\ell}\gamma\gamma$	
520	$p\bar{p} \rightarrow Z\gamma\gamma \rightarrow \ell^-\ell^+\gamma\gamma$	
521	$p\bar{p} \rightarrow Z\gamma\gamma \rightarrow \nu_{\ell}\bar{\nu}_{\ell}\gamma\gamma$	
530	$p\bar{p} \rightarrow \gamma\gamma\gamma$	
610	$p\bar{p} \rightarrow W^-\gamma j \rightarrow \ell^-\bar{\nu}_{\ell}\gamma j$	} anomalous couplings
620	$p\bar{p} \rightarrow W^+\gamma j \rightarrow \ell^+\nu_{\ell}\gamma j$	
630	$p\bar{p} \rightarrow W^-Zj \rightarrow \ell_1^-\bar{\nu}_{\ell_1}\ell_2^-\ell_2^+j$	
640	$p\bar{p} \rightarrow W^+Zj \rightarrow \ell_1^+\nu_{\ell_1}\ell_2^-\ell_2^+j$	
800	$p\bar{p} \rightarrow W^+\gamma\gamma j \rightarrow \ell^+\nu_{\ell}\gamma\gamma j$	
810	$p\bar{p} \rightarrow W^-\gamma\gamma j \rightarrow \ell^-\bar{\nu}_{\ell}\gamma\gamma j$	

The processes accessed via the executable `ggflo` are given below.

PROCID	PROCESS	BSM
4100	$p\bar{p}^{(-)} \rightarrow H jj$	MSSM, general 2HDM
4101	$p\bar{p}^{(-)} \rightarrow H jj \rightarrow \gamma\gamma jj$	} MSSM
4102	$p\bar{p}^{(-)} \rightarrow H jj \rightarrow \mu^+\mu^- jj$	
4103	$p\bar{p}^{(-)} \rightarrow H jj \rightarrow \tau^+\tau^- jj$	
4104	$p\bar{p}^{(-)} \rightarrow H jj \rightarrow b\bar{b} jj$	
4105	$p\bar{p}^{(-)} \rightarrow H jj \rightarrow W^+W^- jj \rightarrow \ell_1^+\nu_{\ell_1}\ell_2^-\bar{\nu}_{\ell_2} jj$	
4106	$p\bar{p}^{(-)} \rightarrow H jj \rightarrow ZZ jj \rightarrow \ell_1^+\ell_1^-\ell_2^+\ell_2^- jj$	
4107	$p\bar{p}^{(-)} \rightarrow H jj \rightarrow ZZ jj \rightarrow \ell_1^+\ell_1^-\nu_{\ell_2}\bar{\nu}_{\ell_2} jj$	
4300	$gg \rightarrow W^+W^- \rightarrow \ell_1^+\nu_{\ell_1}\ell_2^-\bar{\nu}_{\ell_2}$	} anomalous HVV couplings
4330	$gg \rightarrow ZZ \rightarrow \ell_1^-\ell_1^+\ell_2^-\ell_2^+$	
4360	$gg \rightarrow Z\gamma \rightarrow \ell_1^-\ell_1^+\gamma$	
4370	$gg \rightarrow \gamma\gamma$	